

Spatially Dependent Self-Shielding Method with Temperature Distribution for LWR Lattice Physics Code PARAGON

Hideki Matsumoto^{*1}, Mohamed Ouisloumen², Takako Shiraki¹, Kazuya Yamaji¹
and
Toshikazu Takeda³

¹Mitsubishi Heavy Industries, Ltd.: 3-3-1 Nishu-ku, Yokohama, 220-8401 Japan

²Westinghouse Electric Company: Pittsburgh, PA 15230-0355 USA,

³Osaka University: Yamada-oka 2-1 Suita, Osaka 565-0871 Japan

Abstract

The power distribution within the fuel rod is usually needed in fuel integrity evaluation. To compute the radial power distribution, a multi-ring flux solver, a space dependent resonance self-shielding module and a multi-ring depletion module are required. Conventional LWR design codes have almost all of the functions except for the space dependent resonance shielding. Therefore, we had developed SDDM (Spatially Dependent Dancoff Method) and validated the method with Monte Carlo calculations and PIE data. However, the evaluation with the SDDM lacked the temperature distribution within fuel rods. In this paper, the new development of the SDDM with temperature distribution is presented.

The preliminary study for the SDDM with temperature distribution was previously discussed in reference [3]. Then it was found that the SDDM predicts a much larger reactivity effect due to the temperature distribution than MCNP. Here, the improvement to the SDDM corrects this overprediction and it will be supported by numerical results.

KEYWORDS: *SDDM, Spatially Dependent Dancoff Method, Fuel Integrity Evaluation, Power Distribution within Fuel Rod, LWR Lattice Physics Code*

1. Introduction

The Spatially dependent Dancoff method (SDDM) was developed to evaluate the power distribution within a fuel rod that has the spatial variation of isotopic contents [1]. The radial power distribution is needed for the fuel integrity evaluation.

The SDDM module, the micro-depletion module and the multi-region flux solver of the PARAGON code have been validated and verified by comparison with the Monte Carlo calculations and measurements [2].

In this study, the SDDM equation is enhanced to be able to handle the temperature profile distribution. The preliminary results of this methodology were presented in reference [3]. At that time, the inner power distribution obtained from PARAGON with SDDM [4,5] agreed very well

* Corresponding author, Tel. +81-45-224-9607, Fax. +81-45-224-9971, E-mail: hideki_matsumoto@mhi.co.jp

with MCNP [6] results. The Doppler defect from hot-zero-power (HZZ) to hot-full-power (HFP) conditions in a typical PWR was also well predicted with SDDM compared to Monte Carlo calculations. However, the reactivity effect of SDDM due to radial temperature distribution was much larger than MCNP: SDDM gave 0.2%Δk but MCNP shows almost no reactivity difference.

Usually in the routine design calculation, one fuel region with flat temperature is applied. To make the calculation accurate, the flat temperature is corrected to reproduce the reactivity with detail modeling. The corrected temperature is called the effective temperature. Going back to the discussion in the previous paragraph, the SDDM result needed 200pcm correction. That corresponds to about 60(K). The correction is too large to be applied because it is well known in the literature that the correction of the effective temperature should be less than about 20(K). Therefore, the SDDM needs to be improved for the reactivity inconsistency.

2. Spatially Dependent Dancoff Method

2.1 Derivation of the SDDM Equation with Temperature Distribution

Since the detail derivation of the SDDM theory has already been published in Ref. [2], the idea of treating the temperature distribution will require a thorough investigation [7].

In the SDDM, the blackness of a concentric fuel ring is generated by the following equation

$$\gamma_i = \gamma(\rho_i) - \gamma(\rho_{i-1}) = (\gamma_{BC}^i - \gamma_{AB}^i) - (\gamma_{BC}^{i-1} - \gamma_{AB}^{i-1}) \quad (1).$$

The meanings of the notations are shown in Fig.1. If the pellet has a temperature distribution, it becomes difficult to show the blackness for each region. However, if one wants to get the blackness of ring region “i”, it can be easily obtained by:

$$\gamma_i = \{\gamma_{BC}^i(T_i) - \gamma_{AB}^i(T_i)\} - \{\gamma_{BC}^{i-1}(T_i) - \gamma_{AB}^{i-1}(T_i)\} \quad (2).$$

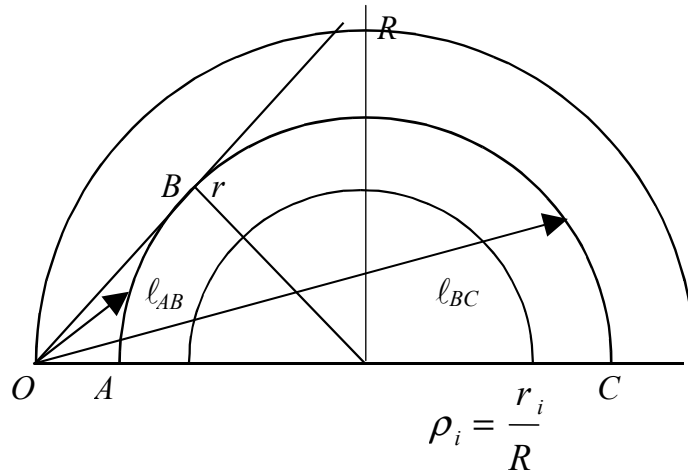
Whatever temperature distribution the pellet has, the regions other than the target ring “i” cancel out each others. Therefore, one can assume that the pellet has the flat temperature of the targeted ring. Based on this assumption, the SDDM equation can be easily derived as,

$$\sigma_{x,i}^g(T_i) = \frac{\sum_{m=1}^4 F_m \sum_{n=1}^2 \beta_n I_{x,g}^k(\sigma_b^{nmk}, T_i)}{1 - \sum_{m=1}^4 F_m \sum_{n=1}^2 \beta_n \frac{I_{a,g}^k(\sigma_b^{nmk}, T_i)}{\sigma_b^{nmk}}} \quad (3)$$

$$\sigma_b^{nmk} = \frac{\Sigma_b + \alpha_n / \ell_m}{N_k} \quad (4)$$

where Σ_b is the background cross-section of the fuel lump and N denotes number density, and k, g, a and i denote nuclide, energy-group, absorption and ring-number, respectively. The function F_m is described in Table 1.

Figure 1: Illustration of chord lengths used in SDDM. The blackness of the regions OAB and OBC are generated with the chord lengths of ℓ_{AB} and ℓ_{BC} .



$$\ell_{AB} = \frac{2R}{\pi} \left(\sqrt{1-\rho^2} + \frac{1}{\rho} \sin^{-1} \rho - \frac{\pi}{2} \rho \right) \quad \ell_{BC} = \frac{2R}{\pi} \left(\sqrt{1-\rho^2} + \frac{1}{\rho} \sin^{-1} \rho + \frac{\pi}{2} \rho \right)$$

Table 1: Definition of the function F_m

m	ℓ_m	F_m
1	$\ell_{BC}(\rho_i)$	$\frac{S_0 \rho_i \ell_{BC}(\rho_i)}{4V_i}$
2	$\ell_{AB}(\rho_i)$	$-\frac{S_0 \rho_i \ell_{AB}(\rho_i)}{4V_i}$
3	$\ell_{BC}(\rho_{i-1})$	$-\frac{S_0 \rho_{i-1} \ell_{BC}(\rho_{i-1})}{4V_i}$
4	$\ell_{AB}(\rho_{i-1})$	$\frac{S_0 \rho_{i-1} \ell_{AB}(\rho_{i-1})}{4V_i}$

S_0 : fuel pellet surface, BC and AB denote OAB and OBC as shown in Fig.1

2.2 Modification of the SDDM using Monte Carlo Calculation

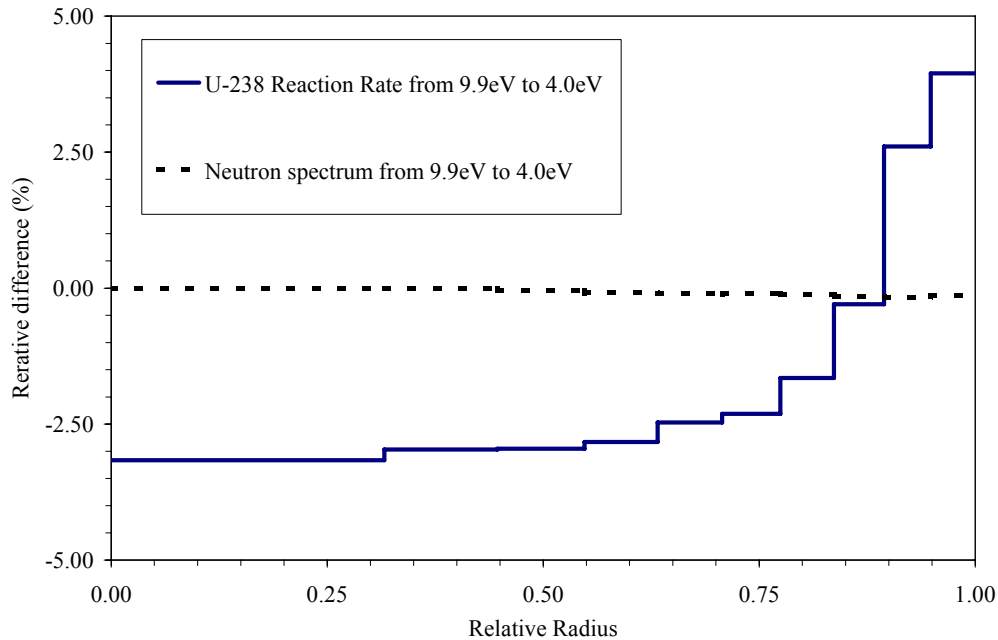
2.2.1 Detail Edits obtained with MCNP

The absorption rate distribution within a fuel rod was evaluated by using MCNP4C. The temperature was assumed to be at the full power operation condition. The fuel rod was divided into 10 equal volume rings. To demonstrate the temperature distribution model, each cross-section set for each ring region was generated using NJOY99. Tally of the ^{238}U absorption rate from about

9eV to 4eV in the temperature distribution case was compared to that in the flat temperature case. The integrated flux from 9eV to 4eV was also compared between the two cases. Those relative differences are shown in Fig.2.

It can be seen from the Fig.2 that the absorption rate changes due to temperature distribution. In peripheral region, the temperature in the profile case becomes smaller than that in flat case. Therefore, the peripheral absorption rate in the profile case becomes smaller than that in flat case due to Doppler broadening. In the center regions, the opposite trends are observed.

Figure 2: Comparisons of ²³⁸U absorption rate and neutron flux ranging from 9.9eV to 4.0eV between temperature distribution model and flat temperature model. A typical temperature distribution within a rod at a 3-loop PWR full power condition is assumed. In the flat case, the volume average temperature is used.



2.2.2 Improved SDDM equation

The SDDM equation is given by Eq.(3) can be modified to be consistent with the Monte Carlo results. The numerator in the Eq.(3) stands for the reaction rates. Each term has temperature dependency. Theoretically this agrees with the MCNP results. The question is the denominator of the Eq.(3) which stands for neutron flux. Since the current SDDM employs temperature dependent resonance integral, the neutron flux becomes dependent on the temperature. However, MCNP shows that the neutron flux is constant. This could be coming from the two-term rational approximation that this module uses (ie more terms are needed to converge to an asymptotic value). Therefore, to be consistent with MCNP, SDDM should employ the average temperature in the denominator of the Eq.(3) as below.

$$\sigma_{x,i}^g(T_i) = \frac{\sum_{m=1}^4 F_m \sum_{n=1}^2 \beta_n I_{x,g}^k(\sigma_b^{nmk}, T_i)}{1 - \sum_{m=1}^4 F_m \sum_{n=1}^2 \beta_n \frac{I_{a,g}^k(\sigma_b^{nmk}, T_{Avg})}{\sigma_b^{nmk}}} \quad (5)$$

3. Numerical Results

3.1 Reactivity Comparison

Pin cell calculations were performed to validate the improved SDDM (ISDDM). A typical cell model was used. It has 1.33cm cell pitch, 0.41 fuel radius and 0.48 cladding radius. The enrichment of the fuel is 4.1wt%. The temperature distribution corresponds to a typical 3-Loop PWR full power condition. Table 2 shows the comparison among SDDM, ISDDM, which are both implemented in PARAGON, and MCNP results. In ISDDM case, two types of average temperature are used. One is the volume average temperature and the other is the chord average temperature [8]. If one uses the volume average temperature, ISDDM shows no reactivity effect as expected. But, if one uses the chord average temperature, ISDDM shows almost same reactivity effect as MCNP4C.

Table 3 shows the reactivity changes between two different liner power densities by using different spatial flux and spatial temperature modeling. It can be seen that k-infinities are in very good agreement within 0.02%Δk. The reactivity changes are also in very good agreement within 1%.

Table 2: Comparison of the effect due to temperature distribution change from flat to parabolic profile.

	PARAGON			MCNP4C
	SDDM	ISDDM(a)	ISDDM(b)	
Reactivity (pcm)	142	5	58	51 (1σ:10)

(a) The volume average temperature is used in the denominator of the equation (5).

(b) The chord average temperature is used in the denominator of the equation (5).

Table 3: Comparison of k-infinities among different space and temperature models. All calculations were performed with PARAGON with ISDDM. These cases correspond to one-region fuel model, multi-ring fuel model with flat temperature and multi-ring fuel model with parabolic temperature distribution, respectively. The chord average temperature is used for the flat temperature and for the denominator of the ISDDM equation (Eq.(5)).

	Flat Flux Flat Temperature	Spatial Flux Flat Temperature	Spatial Flux Spatial Temperature
19.29kW/m	1.38179	1.38195	1.38202
28.02kW/m	1.37612	1.37633	1.37640
Reactivity Difference(%)	0.412	0.408	0.408

3.2 Absorption Rate Distribution Comparison

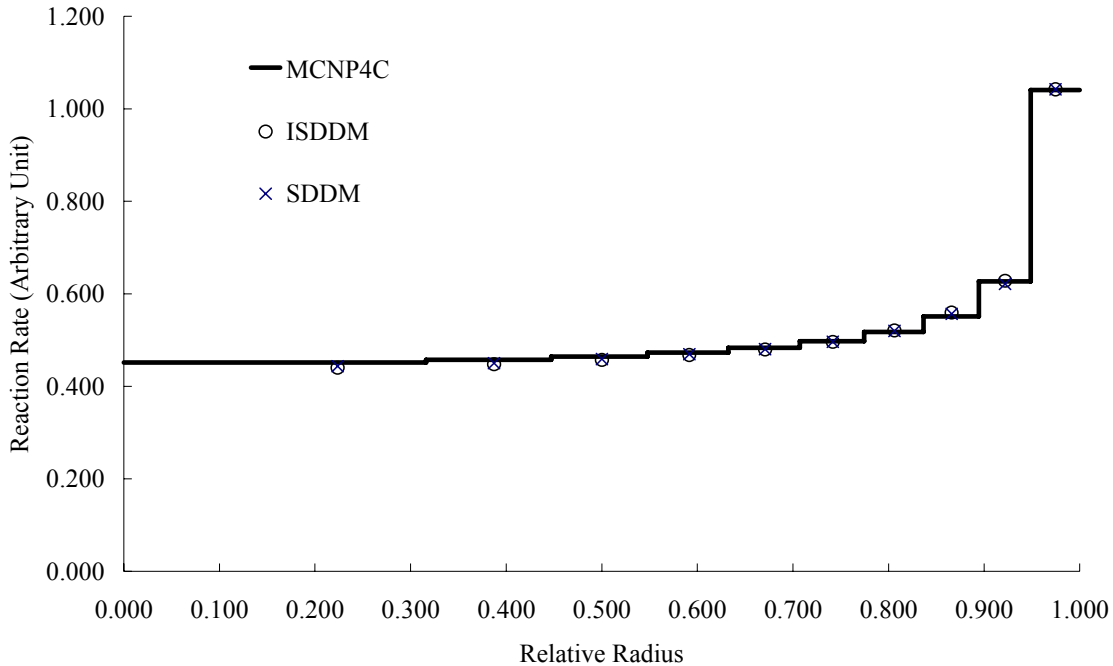
The absorption rate distributions obtained from PARAGON(SDDM), PARAGON(ISDDM) and MCNP were compared in Fig.3. It can be seen that both PARAGON results agree well with Monte Carlo result. This means that ISDDM doesn't affect reaction rate distribution. It had already been reported that the results of PARAGON with SDDM agreed very well with MCNP and PIE measurements. Therefore, the PARAGON with ISDDM has the same applicability as the PARAGON with SDDM.

4. Conclusion

The Spatially Dependent Dancoff method, SDDM, was improved to treat temperature distribution within a rod correctly. The improved SDDM is validated by comparison to continuous energy MCNP4C reactivity and reaction rate distribution results.

ISDDM has to be used together with volume average temperature or chord average temperature. With the chord average temperature, the reactivity change of PARAGON with ISDDM due to temperature distribution agreed better with MCNP4C. On the other hand, ISDDM gave almost same reaction rate distribution as SDDM. Both results are in good agreement with MCNP result.

Figure 3: Comparison of U-238 absorption rate distribution within a typical 4.1wt% UOX rod. Both ISDDM result and SDDM result were obtained with PARAGON code.



Acknowledgements

The author (H.M) wishes to thank Mr.Nakano and Mr.Komano of Mitsubishi Heavy Industries, Ltd. for their valuable advice and help.

References

- 1) H. Matsumoto, et al., "Comparison of resonance shielding methods for application to PWR core design," Proc. Int. Conf. on Advances in Reactor Physics and Mathematics and Computation into the Next Millennium, PHYSOR2000, Pittsburgh, Pennsylvania, USA, 3502 (2000).
- 2) H. Matsumoto, et al., "Development of Spatially Dependent Resonance Shielding Method," J. Nucl. Sci. Technol., 42[8], 688-694(2005).
- 3) H. Matsumoto, et al., "Spatially and Temperature Dependent Dancoff Method for LWR Lattice Physics Code," Proc. Int. Conf. on the Physic of Fuel Cycles and Advanced Nuclear Systems: Global Developments, PHYSOR2004, Chicago, Illinois, USA (2004)
- 4) M. Ouisloumen, et al., "PARAGON: The new Westinghouse lattice code," Proc. ANS Int. Meeting on Mathematical Methods for Nuclear Applications, Sept. 2001, Salt Lake City, Utah, USA, (2001)
- 5) M. Ouisloumen, et al., "The new lattice code PARAGON and its qualification for PWR core applications," Proc. Int. Conf. on Supercomputing in Nuclear Applications, SNA'2003, Sept.

2003, Paris, France, (2003)

- 6) Los Alamos National Laboratory, Los Alamos, New Mexico "MCNP4C: Monte Carlo N-Particle Transport Code System," CCC-700 (2000)
- 7) H. Matsumoto, et al., "Spatially Dependent Self-Shielding Method with Temperature Distribution for The 2-Dimensional Transport code PARAGON," submitted to J. Nucl. Sci. Technol.
- 8) W.J.M. de Kruijf, et al. "The Effective Temperature to be Used for Calculating Resonance Absorption in a $^{238}\text{UO}_2$ Lump with Nonuniform Temperature Profile," Nucl. Sci. Eng., **vol.123**, 121-135(1996)